Carbohydrate Polymers 80 (2010) 1018–1027

Contents lists available at ScienceDirect

Carbohydrate Polymers

journal homepage: www.elsevier.com/locate/carbpol

Nicotine-loaded sodium alginate–magnesium aluminum silicate (SA–MAS) films: Importance of SA–MAS ratio

Thaned Pongjanyakul *, Hatairat Suksri [1]

Faculty of Pharmaceutical Sciences, Khon Kaen University, Khon Kaen 40002, Thailand

ARTICLE INFO

Article history:
Received 30 November 2009
Received in revised form 8 January 2010
Accepted 8 January 2010
Available online 15 January 2010

Keywords:
Sodium alginate
Magnesium aluminum silicate
Nicotine
Release mechanism
Drug permeation
Mucosal delivery

ABSTRACT

The objective of this work was to investigate the influence of the sodium alginate–magnesium aluminum silicate (SA–MAS) ratio on film properties for nicotine (NCT) mucosal delivery. NCT-loaded SA–MAS films with varying SA–MAS ratios were prepared at acidic and basic pH, which represent the protonated and neutral species of NCT, respectively. The film characteristics, such as NCT content, muco-adhesive properties, NCT release and skin and mucosal membranes NCT permeation were examined. The result showed that increasing the MAS ratio in the films caused an increase in NCT retention and a decrease in the NCT release rate. The NCT release mechanism of the NCT-loaded SA–MAS films prepared at acidic and basic pH was an anomalous transport and a swelling controlled mechanism, respectively, and was primarily impacted by the SA content in the films. The NCT permeation rate across the mucosal membrane decreased with increasing MAS ratio of the films. The mucosal drug permeation kinetics suggested a matrix diffusion controlled mechanism, whereas skin penetration acted as a rate-limiting step of drug permeation. Film preparation pH also affected NCT release and permeation due to the unique charge characteristics of the various NCT species formed. Furthermore, films with a high MAS ratio could adhere to the mucosal membrane. These findings suggest the SA–MAS ratio remarkably influences the characteristics of the NCT-loaded SA–MAS films, and that these films demonstrate a promising mucosal drug delivery system.

1. Introduction

Polymer–clay composites have been interestingly developed and characterized for their mechanical properties and their ability to improve polymer thermal behavior (Pavlidou & Papaspyrides, 2008). Changes in the physicochemical properties of polymers occur when clay is incorporated due to molecular interactions between the polymer and clay. This incorporation leads to an alteration of polymer matrix structure, which may slow drug release. For this reason, the polymer–clay composites with drugs incorporated have been studied for drug delivery systems (Campbell, Craig, & McNally, 2008; Stephen, Mark Saltzman, & Giannelis, 2003; Tammaro, Costantino, Nocchetti, & Vittoria, 2009; Wang, Du, Luo, Lin, & Kennedy, 2007).

Composites between sodium alginate (SA) and magnesium aluminum silicate (MAS) are materials that possess unique characteristics for pharmaceutical use (Aguzzi, Cerezo, Viseras, & Caramella, 2007; Lee, Moturi, & Lee, 2009). SA is a sodium salt of alginic acid, a natural polysaccharide found in marine brown algae. SA has been widely used as a food and pharmaceutical additive, a tablet disintegrant, and a gelling agent (Kibbe, 2000). MAS is a mixture of montmorillonite and saponite clays (Kibbe, 2000) with a layered structure. Each layer is constructed from tetrahedrally coordinated silica atoms fused into an edge-shared octahedral plane of either aluminum hydroxide or magnesium hydroxide (Alexandre & Dubois, 2000; Kibbe, 2000). This layered structure of MAS possesses weakly positively charged edges and negatively charged faces. The positively charged edges on the MAS layers interact with SA to form a phase-separated microcomposite. Previous studies investigated the physicochemical properties and the drug and/or water vapor permeability of the SA–MAS composite films (Pongjanyakul, 2009; Pongjanyakul, Priprem, & Puttipipatkhachorn, 2005). Moreover, the SA–MAS composite dispersions were tested as a coating material for tablets and shown to effectively modulate drug release from the tablets (Pongjanyakul et al., 2005).

Nicotine (NCT), obtained from tobacco plants, is a volatile and strongly alkaline liquid. It has two well-separated pK_a values (pK_{a1} of 3.04 and pK_{a2} of 7.84), which cause the formation of diprotonated, monoprotonated, and neutral NCT species at acidic, neutral, and basic pH, respectively (Nair, Chetty, Ho, & Chien, 1997). Common NCT delivery sites are the skin and mucosal membranes, such as buccal and nasal mucosae, because both the neutral and protonated NCT forms can readily permeate the mucosal membrane (Chen, Chetty, & Chien, 1999; Nair et al., 1997). Due to the volatile liquid

* Corresponding author. Tel.: +66 43 362092; fax: +66 43 202379.
E-mail address: thaned@kku.ac.th (T. Pongjanyakul).
[1] Present address: Sirindhorn College of Public Health, Khon Kaen 40000, Thailand.

0144-8617/$ - see front matter © 2010 Elsevier Ltd. All rights reserved.
doi:10.1016/j.carbpol.2010.01.019

and oxidative degradation of the free base form of NCT, several researchers are seeking a material to adsorb the basic form of NCT to prevent evaporation and improve stability. Previously tested materials for NCT adsorption include cellulose powder (Mihranyan, Andersson, & Ek, 2004) and cation exchange resins (Borodkin, 1993; Cheng et al., 2000). Recently, the interaction between NCT and MAS at varying pH was also investigated. This composite led to the adsorption of NCT onto MAS particles and formation of NCT–MAS flocculates (Suksri & Pongjanyakul, 2008). The dry powder of NCT–MAS complexes could produce a sustained NCT release pattern in physiological fluids following mucosal administration (Pongjanyakul, Khunawattanakul, & Puttipipatkhachorn, 2009).

We recently tested SA–MAS films with a ratio of 1:1 at different pH. These composites demonstrated the potential to provide a film matrix for NCT delivery, especially through transmucosal delivery. The protonated and neutral NCT species could interact with the negatively charged MAS to form numerous NCT–MAS complexes that acted as microreservoirs in the films. This reservoir generation led to a reduction in NCT evaporation during film drying and sustained NCT release and mucosal membrane NCT permeation (Pongjanyakul & Suksri, 2009). Several researchers have also studied the effects of clay content on the physical properties of the polymer–clay composite films (Sothornvit, Hong, An, & Rhim, 2010; Magalhães & Andrade, 2009). Therefore, MAS content may affect the characteristics of the NCT-loaded SA–MAS films, particularly NCT retention in the films, NCT release kinetics and NCT permeation of the skin and mucosa.

The objective of this work was to study the influence of the SA–MAS ratio on the film characteristics of NCT-loaded SA–MAS films. The NCT-loaded SA–MAS films were prepared at pH 5 and 10, which represented the protonated and neutral NCT species, respectively. Film preparations were made by following a casting/solvent evaporation method. The surface morphology, internal structure, NCT content and muco-adhesive properties of the films were investigated. Furthermore, the NCT release and permeation across shed snake skin (a model skin) and porcine esophageal epidermis (a model mucosa) were also examined.

2. Materials and methods

2.1. Materials

MAS (Veegum®HV) and NCT (liquid state and free base form) were obtained from R.T. Vanderbilt Company Inc. (Norwalk, CT, USA) and Fluka (Buchs, Switzerland), respectively. SA (Manugel®DMF) was obtained from ISP Thailand Ltd. (Bangkok, Thailand). All other reagents used were analytical grade and used as received.

2.2. Preparation of the NCT-loaded SA–MAS films

The NCT-loaded SA–MAS films were prepared with SA–MAS ratios of 1:0.25, 1:0.5, and 1:1. The solid content in the dispersion for film casting was a total of 3 g of materials. The SA was initially dispersed in 100 ml of distilled water to obtain a homogeneous dispersion; subsequently the MAS was pre-hydrated with 100 ml of hot water and then added to the SA suspension. The composite dispersions were then mixed for 5 min at 5000 rpm using a homogenizer (Ystral T1500, Dottingen, Germany). NCT (0.3 g, 10% of the solid content in the dispersion) was subsequently added to the composite. The pH of the SA–MAS dispersion containing NCT was adjusted by titration with either 1N HCl or 1N NaOH. The final solution pH of either 5 or 10 was verified with a pH meter (Ion Analyzer 250, Coring, USA). After pH titration, the composite dispersions were adjusted to a final volume of 300 ml with distilled water. The dispersions were then mixed and incubated at 37 °C for 24 h. The dispersions with NCT at SA–MAS ratios of 1:0.25 and 1:0.5 by weight were also prepared using the same procedure as mentioned above. Two-hundred and fifty milliliters of each of the SA–MAS dispersions with NCT at different pH was poured onto a plastic plate (15 cm × 20 cm) and allowed to evaporate at 50 °C for 24 h. The films were peeled off and stored in a desiccator (40 ± 2% RH).

To obtain the NCT-loaded SA films, SA (3 g) was dispersed in 200 ml of distilled water and the dispersions were then mixed for 5 min at 5000 rpm using a homogenizer. NCT (0.3 g, 10% of solid content in the dispersion) was then added to the SA dispersions. The pH of the SA dispersion with NCT was adjusted by adding a small amount of 1N HCl or 1N NaOH with stirring, while monitoring with a pH meter until the final pH of the dispersions was 5 or 10. After that, the dispersion was adjusted to a final volume of 300 ml with distilled water and incubated at 37 °C for 24 h before use. The film casting of the SA dispersion with NCT was done using the methods described above.

2.3. Determination of film thickness

The films were placed on a control plate and the film thickness was measured in 20 places using a microprocessor coating thickness gauge (Minitest 600B, ElektroPhysik, Germany). The probe was connected to a measurement gauge and calibrated using a standard film.

2.4. Determination of NCT content

The films (0.98-cm diameter) were cut and weighed. Discs were soaked in 50 ml of 2N HCl and incubated at 37 °C with intermittent shaking for 24 h (Pongjanyakul & Suksri, 2009). The solution was collected, filtered using a 0.45-μm cellulose acetate membrane and analyzed with a UV–visible spectrophotometer at a wavelength of 259 nm (Shimadzu UV1201, Japan). The NCT content was calculated as the percentage by weight.

2.5. Surface morphology and internal structure of the films

The surface morphology and internal structure of the films was observed by scanning electron microscopy (SEM). For internal structure studies, the films were immediately fractured after immersion in liquid nitrogen for 2 s. The films were mounted onto stubs, sputter coated with gold in a vacuum evaporator and photographed using a scanning electron microscope (Jeol Model JSM-6400, Tokyo, Japan).

2.6. In vitro release studies

A 6 ml modified Franz-diffusion cell (1-cm diameter) was used and the receptor solution (pH 5.6 citrate–phosphate buffer solution (CPBS) at 37 °C) was stirred at 600 rpm. A piece of 0.45-μm cellulose acetate (Sartorius Stedim Biotech Gmbh, Germany) was used as a membrane for release testing. The membrane was soaked in CPBS overnight and then mounted on a diffusion cell. The films (0.68-cm diameter) were placed on the hydrated membrane and the cells were fixed and tightly fastened with a clamp. At appropriate intervals, 0.4 ml aliquots of the receptor solution were withdrawn and immediately replaced by fresh solution. The concentration of NCT in the receptor medium was collected and analyzed via HPLC.

The total time until 25% NCT content release ($T_{25\%}$) was calculated to compare NCT film release rates. The mechanism of NCT release was determined by using a semi-empirical equation or the power law as follows (Peppas, 1985; Siepmann & Siepmann, 2009):

$$\frac{M_t}{M_\infty} = kt^n \quad (1)$$

$$\mathrm{Log}\frac{M_t}{M_\infty} = n\log t + \log k \quad (2)$$

where M_t/M_∞ is the fractional NCT release at time t, k is the kinetic constant, and n is the release exponent, which is indicative of the drug release mechanism. For thin films, a release exponent of $n = 0.5$ indicates a diffusion-controlled drug release, whereas a release exponent of $n = 1$ corresponds to a purely polymer swelling-controlled release mechanism. Thus, release exponents between these two extreme values indicate a complex transport mechanism that is a mixture of both drug diffusion and polymer swelling (Ritger & Peppas, 1987).

2.7. In vitro permeation studies

Barrier membranes used to model skin and mucosal membranes were the shed skin of a king cobra (*Ophiophagus hannah*) and porcine esophagus mucosa, respectively. The apparatus used was the same as for release testing mentioned in Section 2.6. The shed king cobra skin was a gift from the King Cobra Village (Khon Kaen, Thailand). The cobra skin was washed with distilled water and dried at room temperature. The dorsal portion of the skin was cut into an appropriate size and stored at −20 °C until needed. The porcine esophageal mucosa was obtained from a local slaughterhouse (Non Muang Village, Khon Kaen, Thailand). The porcine esophageal tube was opened longitudinally and immersed in a pH 7.4 isotonic phosphate buffer solution (PBS) at 60 °C for 1 min (Diaz del Consuelo, Falson, Guy, & Jacques, 2007; Diaz del Consuelo, Jacques, Pizzolato, Guy, & Falson, 2005). The epithelium was peeled away from the connective tissue and then frozen at −20 °C until further use. Frozen membranes were brought to room temperature and pre-hydrated in PBS was 30 min (for the pig mucosal membranes) and 12 h (for the shed snake skin). The prepared membrane was then mounted on a diffusion cell that contained a PBS receptor solution. Twenty microliters of CPBS was spread over the membranes and the films were then placed on a hydrated membrane; the cells were then fixed and tightly fastened with a clamp. Sampling of the receptor medium and NCT analysis was performed using the same method as the release study.

2.8. HPLC analysis

The concentration of NCT was determined by HPLC analysis (Agilent 1000 series, Agilent Technologies, USA). A Reversed-phase C-18 column (HiQ Sil C18V, 4.6 × 250 mm) with a guard column was connected to the HPLC apparatus. The mobile phase was 0.05 M sodium acetate:methanol:triethylamine (88:12:0.5 v/v), with a final pH of 4.2 (adjusted with glacial acetic acid). The flow rate of mobile phase was 1 ml min^{-1}, and samples were detected at a wavelength of 259 nm using a UV–visible spectrophotometric detector. The retention time of NCT was approximately 6.6 min. Under these conditions, linearity and reproducibility were seen over the range of 0.1–400.0 μg ml^{-1} NCT.

2.9. Muco-adhesive properties

A modified in-house pulley system previously described by Wittaya-areekul and Prahsarn (2006) was used to assess the muco-adhesive properties of the films. The porcine esophageal tube (mucosal membrane) was soaked in PBS and opened longitudinally. The esophageal mucosa (measuring 4 cm × 4 cm) was attached to the platform. Twenty microliters of CPBS was spread over the mucosal membrane to simulate fluid. A film (measuring 1 cm × 1 cm) was attached to the mucosa with a weight of 20 g for 1 min, while the other side was attached to a platform connected to a pulley system. Distilled water was then added to a water container connected to the pulley system until the wet film was separated from the mucosa. The total weight of the distilled water needed for separation was recorded as detachment force per cm^2.

3. Results and discussion

3.1. Film preparation

The SA dispersions had a neutral pH while a higher pH was observed following NCT incorporation. Therefore pH adjustment to 5 and 10 required the use of hydrochloric acid and sodium hydroxide solutions, respectively. The SA dispersion with NCT at pH 10 provided a homogeneous dispersion, whereas the pH 5 dispersion did not. This difference in dispersion was likely due to a strong interaction between negatively charged SA and protonated NCT after the addition of hydrochloric acid; thus, we were unable to cast films under these conditions. In contrast, there were no incompatibility issues between NCT and SA in the composite dispersions. It is probable that NCT is adsorbed onto the MAS before pH adjustment and that after hydrochloric acid addition the low pH caused the formation of protonated NCT that possessed a higher affinity for MAS (Suksri & Pongjanyakul, 2008). Therefore, no incompatibility was observed under these conditions.

3.2. SEM studies

The surface morphology of the NCT-loaded SA films showed a smooth surface (Fig. 1a). In contrast, the NCT-loaded SA–MAS films prepared at pH 5 and 10 showed a rougher film surface with increasing MAS content (Fig. 1b–g); these physical characteristics may result from MAS particles and NCT–MAS flocculates. Additionally, the NCT-loaded SA–MAS films prepared at pH 10 displayed a rougher surface than those prepared at pH 5. In fact, a remarkably smaller number of NCT–MAS flocculates were formed at pH 10 compared to pH 5 (Pongjanyakul & Suksri, 2009). For this reason, the larger flocculate size at pH 5 may give a higher rate of sedimentation in the dispersion cast during the drying process. Thus, a smoother surface of the dry films was obtained when preparing the films at acidic pH. The internal morphology of the NCT-loaded SA films demonstrated a dense matrix structure (Fig. 1a). An increase in the MAS ratio caused an obvious change of the internal film structure. The NCT-loaded SA–MAS films with a ratio of 1:1 had a film matrix with a layered structure (Fig. 1f and g). This may be due to embedding of the NCT–MAS flocculates formed in the SA matrix during film formation. However, the results show that the NCT-loaded SA–MAS films prepared at pH 5 and 10 demonstrated no obvious difference in the internal structure morphology, although stronger flocculation of NCT and MAS at pH 5 was observed in our previous study (Pongjanyakul & Suksri, 2009).

3.3. Thickness and NCT content of the films

The NCT-loaded SA films prepared at pH 10 were transparent, whereas the NCT-loaded SA–MAS films prepared at pH 5 and 10 were opaque. The mean thickness of all films ranged between 50 and 60 μm, which is likely due to the constant solid content of the dispersion used for film casting. The NCT content and NCT retained in the prepared pH 5 and pH 10 films are shown in Fig. 2. At pH 10, the NCT-loaded SA–MAS films provided remarkably higher NCT content than the NCT-loaded SA film. The NCT-loaded SA–MAS films at the ratio of 1:0.5 gave greater NCT content than those at

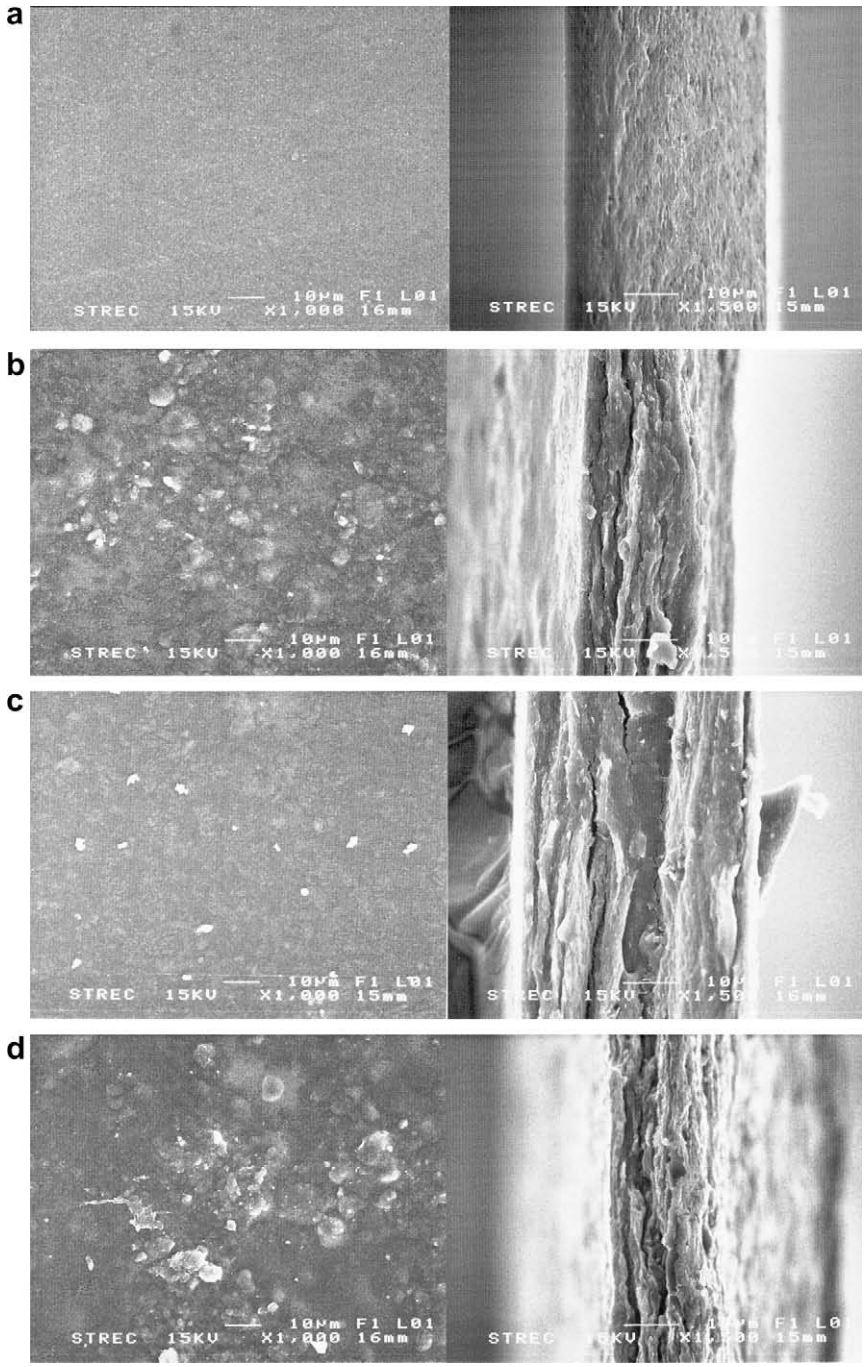

Fig. 1. Micrographs of surface morphology and internal structure of NCT-loaded SA films prepared at pH 10 (a), and NCT-loaded SA–MAS films with ratios of 1:0.25 (b and c), 1:0.5 (d and e), and 1:1 (f and g) prepared at pH 5 and 10, respectively.

1:0.25 ratio, but the NCT-loaded SA–MAS films at the ratios of 1:0.5 and 1:1 gave a similar NCT content. The films prepared at acidic pH showed a higher NCT content than those prepared at basic pH. The highest NCT content was found in the NCT-loaded SA–MAS films at the ratio of 1:1 prepared at pH 5. This resulted in the NCT retained in these films close to 100%.

Due to the volatile nature of basic NCT, the NCT incorporated in the films could evaporate during drying processes at high temperatures. This evaporation led to the lowest NCT content and retained NCT in the NCT-loaded SA films prepared at pH 10, even through the neutral NCT could interact with SA via hydrogen bonding (Pongjanyakul & Suksri, 2009). Incorporation of MAS into the films could retard the evaporation of NCT because of molecular interactions between NCT and MAS (Pongjanyakul et al., 2009), which are dependent on the preparation pH. The electrostatic forces between protonated NCT and MAS were mainly formed at pH 5. Furthermore, the positive charge of protonated NCT can also interact with negatively charged SA. For these reasons, the highest NCT content with non-significant NCT loss was found in the NCT-loaded SA–MAS films at the ratio of 1:1 at pH 5. Decreasing the MAS ratio led to a reduction in NCT–MAS complexes formed, resulting in a higher NCT evaporation and a decrease of NCT content in the films. At pH 10, almost all NCT was present in the neutral form. The neutral NCT could mainly interact with MAS and SA via intermolecular

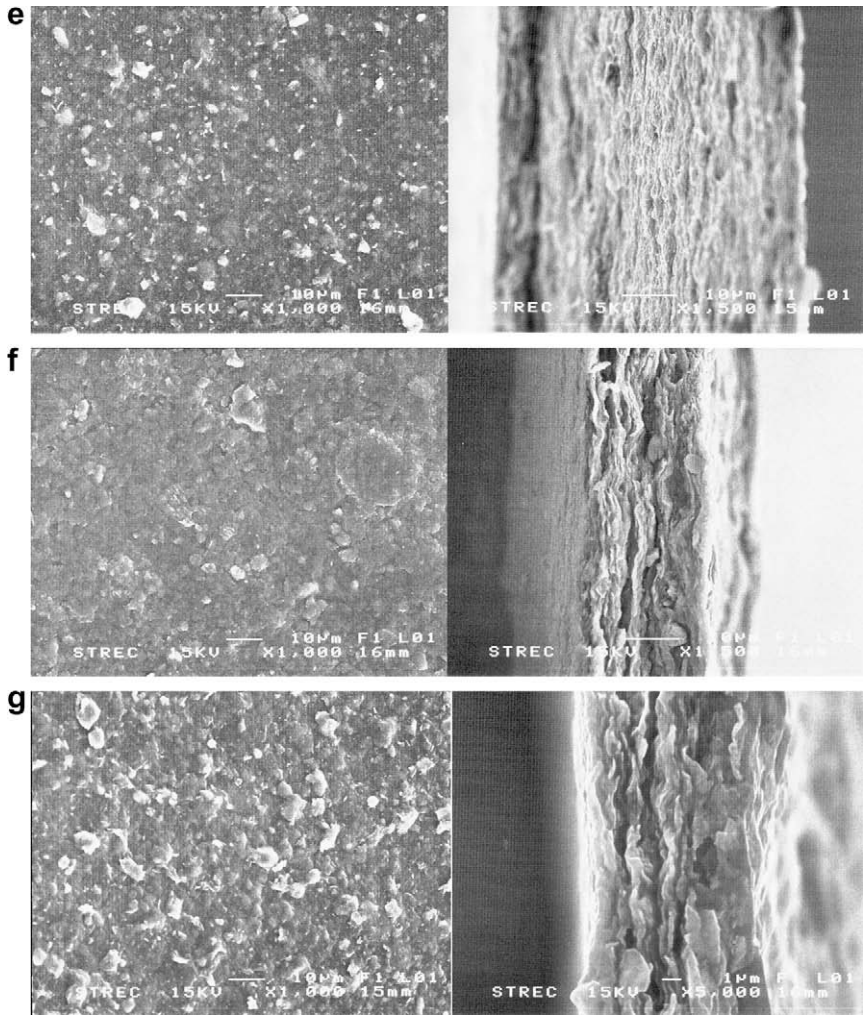

Fig. 1 (*continued*)

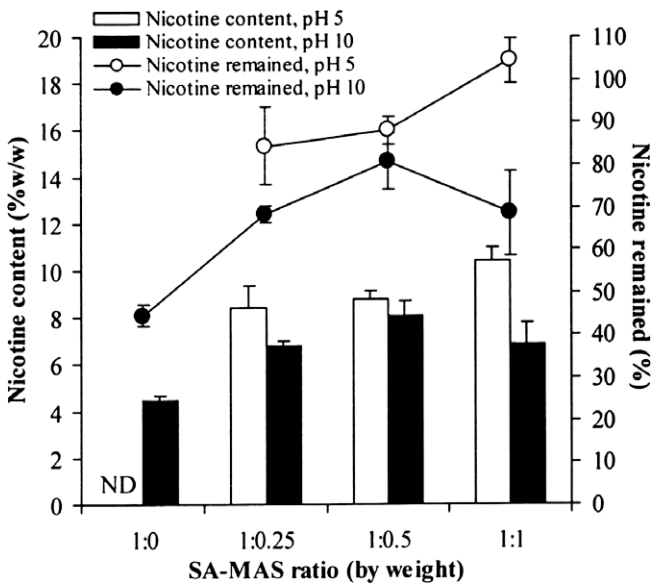

Fig. 2. NCT content and NCT retained in NCT-loaded SA films and NCT-loaded SA–MAS films prepared using various SA–MAS ratios at pH 5 and 10. Each value represents the mean ± SD of an $n = 3$.

hydrogen bonding, although this type of bonding interaction has a weak attraction force when compared to electrostatic interactions. Even though an increase in the MAS ratio could readily adsorb NCT at pH 10, the adsorbed NCT had a greater chance of evaporation because of the weaker hydrogen bonding between the NCT and MAS. This may have led to a similarity in NCT content in the NCT-loaded SA–MAS films at the ratios of 1:0.5 and 1:1 when prepared at pH 10.

3.4. Film NCT release

The NCT release profiles of the pH 5 and 10 films through a cellulose acetate membrane are shown in Fig. 3a and b, respectively. A non-linear curve of NCT release from all films was obtained, suggesting that the rate-limiting step of NCT release was not the diffusion through the membrane, but rather the diffusion within the film matrix. The NCT-loaded SA films yielded obviously faster release rates than the NCT-loaded SA–MAS films at the ratios of 1:0.5 and 1:1. The NCT-loaded SA–MAS films showed a slower and continuous release of NCT after 30 min. The data also show that the total NCT released at 240 min remarkably decreased with increasing MAS ratio in the films. The release rate of the films, expressed as the $T_{25\%}$ value, is shown in Fig. 4a. At pH 10, the $T_{25\%}$ values of the NCT-loaded SA films and the NCT-loaded SA–MAS films

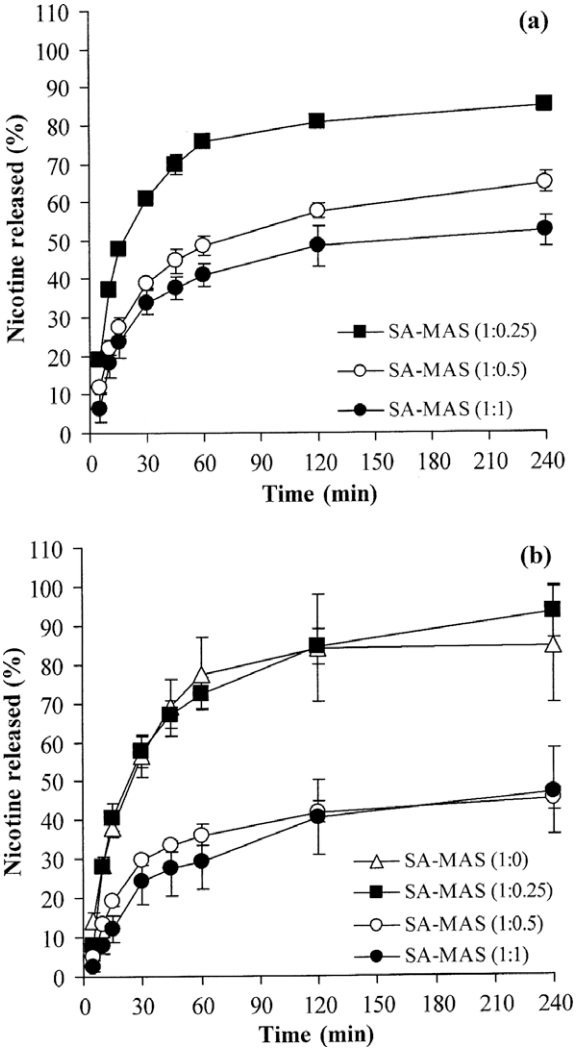

Fig. 3. NCT release profiles of the NCT-loaded SA–MAS films prepared using various SA–MAS ratios at pH 5 (a) and 10 (b). Each value represents the mean ± SD with an $n = 3$.

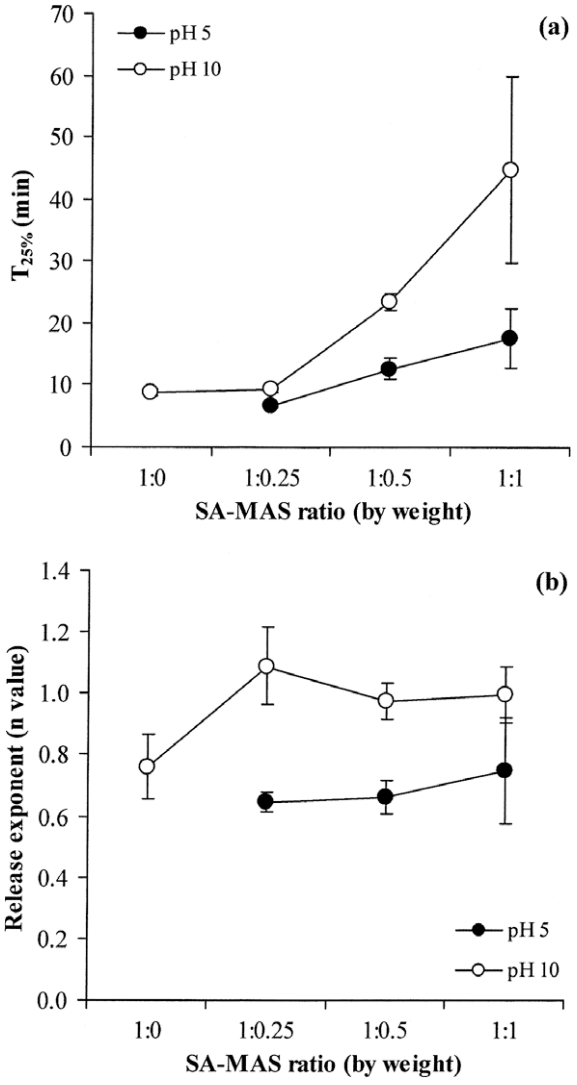

Fig. 4. Effect of SA–MAS ratio on the $T_{25\%}$ value (a) and release exponent (n value) (b) of NCT-loaded SA–MAS films prepared at pH 5 and 10. Each value represents the mean ± SD of an $n = 3$.

at the ratio of 1:0.25 were comparable. Increasing the MAS ratio in the films resulted in a higher $T_{25\%}$ value, indicating a slower NCT release rate. Similar results were seen in the films prepared at pH 5. However, the NCT-loaded SA–MAS films prepared at pH 10 gave slower NCT release rates than those prepared at pH 5, which can be seen from the higher $T_{25\%}$ values of the films prepared at pH 10.

The relationship between $\log M_t/M_\infty$ and $\log t$ showed strong linearity with an R^2 greater than 0.92 over the test range of 5–30 min. The n value, which indicates the NCT release mechanism, of the NCT-loaded SA–MAS films prepared at pH 10 was close to 1 and higher than that of the NCT-loaded SA films (Fig. 4b). In contrast, the NCT-loaded SA–MAS films prepared at pH 5 gave n values that ranged from 0.6 to 0.7. These results suggest a complex mechanism of NCT transport in the films, which is influenced by both NCT diffusion and film swelling controlled NCT release. Moreover, the NCT release from the NCT-loaded SA–MAS films prepared at pH 10 was mainly controlled by film swelling compared to the film prepared at acidic pH. The data also show that the n value was not dependent on the MAS ratio in the films, suggesting that the film swelling is dependent on SA content. Generally, the hydrophilic polymer possesses higher swelling properties than the silicate materials (Wan & Prasad, 1989).

An increase in the MAS ratio of the films caused a decrease in the percentage of NCT released from the films, as well as a slower NCT release rate. This decrease in NCT release was likely due to the high affinity of NCT to MAS and the controlled release of NCT via NCT–MAS complexes embedded in the films; the NCT–MAS complexes were formed at a higher extent with increasing ratios of MAS in the films. Moreover, it is difficult for cations in the solution to exchange with NCT molecules inside of the MAS layers. This ion exchange process may result in the zipping of the crystal edge and a shortening of interlayer distance (Jung, Kim, Choy, Hwang, & Choy, 2008), which can lead to a decrease in NCT release. In this study, the SA matrix of the films was an important factor for modulating the NCT release mechanism. At pH 5, SA was partially converted to alginic acid (an unionized form of SA), whereas all of the SA at pH 10 was an ionized form. This led to an obviously faster swelling of the NCT-loaded SA–MAS film prepared at pH 10 in pH 5.6 CPBS during the first 30 min of release testing when compared with the films prepared at pH 5, which alginic acid could slowly convert to SA in a sodium ion-rich medium. The film swelling caused a longer NCT diffusion path length, leading to a slower NCT release by NCT-loaded SA–MAS films prepared at pH 10. Additionally, a slower NCT release rate by NCT-loaded SA–MAS films

prepared at pH 10 was observed because the lower NCT content in the films created a smaller drug concentration gradient when exposed to the release solution. Thus, the smaller the concentration gradient and the slower the mass transfer resulted in a decreased NCT release rate.

3.5. Film NCT permeation

Shed king cobra skin was used in this study because previous studies have shown that this model skin has similar NCT flux and permeation profiles to human epidermis (Pongjanyakul, Prakongpan, Panomsuk, Puttipipatkhachorn, & Priprem, 2002). The NCT permeation profiles of the NCT-loaded SA–MAS films at the ratio of 1:1 prepared at pH 5 and 10 are compared in Fig. 5a. There was a linear relationship between the percent of NCT permeation and time, indicating skin-controlled permeation with zero-order kinetics. The slope of the linear regression line represents the NCT permeation rate and is listed in Table 1. The NCT permeation rate and amount of NCT permeation of the pH 5 films after 24 h was remarkably lower than pH 10 films (Table 1). It is possible that the NCT released from the films prepared at pH 5 was mostly protonated NCT, which has a lower skin permeability than neutral NCT, the species which predominates at pH 10 (Nair et al., 1997). The effect of the MAS ratio on NCT permeation of the films prepared at pH 10 is presented in Fig. 5b. The NCT-loaded SA film gave the highest NCT permeation rate when compared with the NCT-loaded SA–MAS film (Table 1) and gave the fastest NCT release rate obtained. Incorporation of MAS into the films showed a decrease in NCT permeation rate, which was independent of the MAS ratio. This was likely due to skin-controlled NCT permeation because an increase in NCT release rate did not affect the skin permeation rate. Moreover, the CPBS was added in a small volume, which contained a limited number of cations. This may have restricted cation exchange and led to a smaller amount of NCT release onto the skin surface when compared to the release testing, resulting in no difference of the NCT permeation rate.

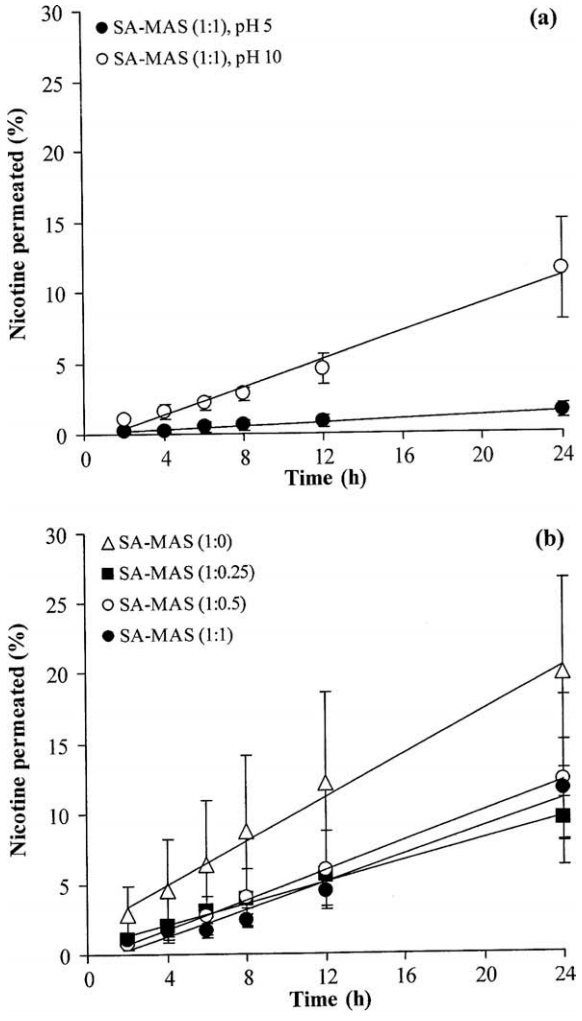

Fig. 5. Effect of preparation pH (a) and of SA–MAS ratio at pH 10 (b) on NCT permeation of NCT-loaded SA–MAS films using shed king cobra skin as a barrier membrane. Each value represents mean ± SD of an $n = 3$.

Table 1
NCT permeation characteristics of SA–MAS films using shed king cobra skin as a barrier membrane.

SA–MAS ratio	NCT permeation rate (% cm^{-2} h^{-1})	Amount of NCT permeated at 24 h (μg cm^{-2})
pH 5		
1:1	0.06 ± 0.02 (R^2 = 0.987)	13.9 ± 5.3
pH 10		
1:0	0.77 ± 0.21 (R^2 = 0.977)	135.4 ± 46.2
1:0.25	0.37 ± 0.08 (R^2 = 0.967)	47.5 ± 7.7
1:0.5	0.52 ± 0.26 (R^2 = 0.992)	84.2 ± 40.9
1:1	0.48 ± 0.16 (R^2 = 0.979)	67.9 ± 21.2

Data are mean ± SD, $n = 3$.

Porcine esophageal mucosa was used as a mucosal membrane because of the previously reported similarities in lipid composition to buccal mucosa (Diaz del Consuelo et al., 2005). Moreover, the esophageal mucosa has also been used in studies to test drug permeability and drug permeation of bioadhesive films (Diaz del Consuelo et al., 2007). The NCT permeation profile of the films with the mucosal membrane is shown in Fig. 6. A non-linear permeation profile of NCT from the films was observed. A clear relationship (R^2 value greater than 0.95) between the percentage of permeated NCT and the square root of time was found over the ranges of 30–480 and 30–120 min for the films prepared at pH 5 and 10, respectively. The NCT permeation parameters of the films are listed in Table 2. The permeated NCT at 30 min and NCT permeation rate decreased with increasing MAS ratios of the films prepared at pH 5 and 10. Both of these parameters were lower in the films prepared at pH 5 than those prepared at pH 10. However, the amount of permeated NCT at 480 min was comparable for the NCT-loaded SA–MAS films prepared at pH 5 and 10 (Table 2). The data indicate that the amount of NCT permeated across the mucosal membrane was obviously higher than that through the shed snake skin (Table 1), indicating a greater NCT permeability of the mucosal membrane.

In this study, a small volume of CPBS (pH 5.6) was added to simulate fluid on the mucosal membrane. When the films were exposed to this solution, NCT was released. Even though released NCT can be converted to the protonated form, the films prepared at pH 10 mainly contained neutral NCT that could rapidly permeate the mucosal membrane. This permeation of the mucosal membrane was influenced not only by the lipoidal pathway, but also by the aqueous pore pathway (Chen et al., 1999; Nair et al., 1997) because of the high aqueous and lipid solubility of the neutral NCT species. On the contrary, protonated NCT at pH 5 had a lower permeability of the mucosal membrane because only the aqueous pore pathway can transport the protonated NCT species (Adrian, Olin, Dalhoff, & Jacobsen, 2006; Chen et al., 1999). This resulted

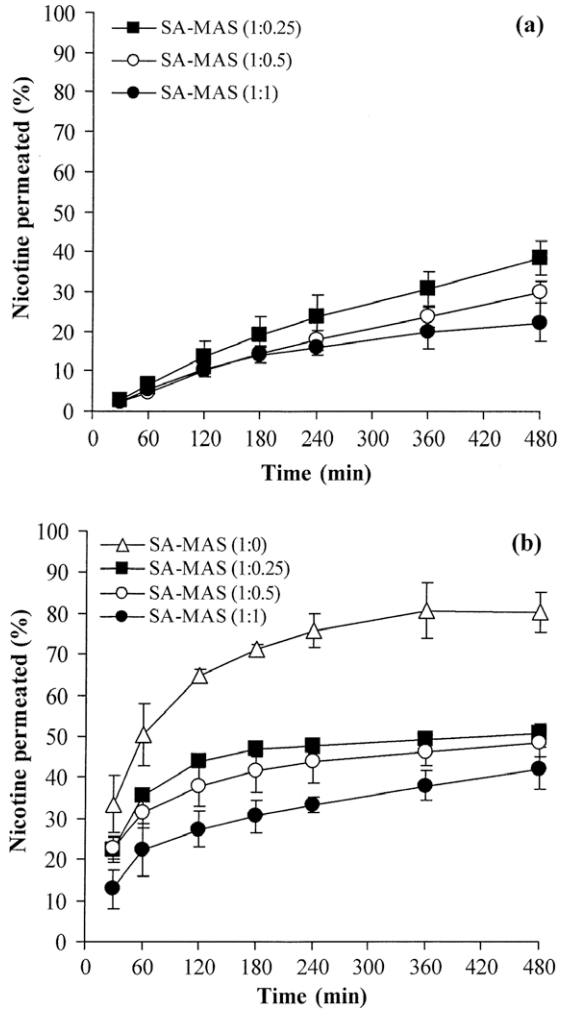

Fig. 6. NCT permeation profiles of NCT-loaded SA–MAS films prepared using various SA–MAS ratios at pH 5 (a) and 10 (b). Each value represents the mean ± SD of an $n = 3$.

in a smaller amount of permeated NCT at 30 min and a slower NCT permeation rate of the films prepared at acidic pH. This may describe a decrease in the NCT permeation rate that was seen with

Table 2
NCT permeation characteristics of SA–MAS films using pig esophagus membrane.

SA–MAS ratio	NCT permeated at 30 min (% cm^{-2})	NCT permeation rate (% cm^{-2} $min^{-0.5}$)	Amount of NCT permeated at 480 min (μg cm^{-2})
pH 5			
1:0.25	2.80 ± 0.67	2.17 ± 0.24 (R^2 = 0.991)	257.5 ± 83.2
1:0.5	2.28 ± 0.11	1.69 ± 0.18 (R^2 = 0.992)	255.9 ± 23.6
1:1	2.41 ± 0.41	1.23 ± 0.29 (R^2 = 0.987)	214.3 ± 46.7
pH 10			
1:0	33.4 ± 7.0	5.61 ± 1.17 (R^2 = 0.977)	546.7 ± 36.5
1:0.25	22.4 ± 3.1	3.87 ± 0.75 (R^2 = 0.949)	256.7 ± 12.8
1:0.5	22.9 ± 3.0	2.28 ± 0.29 (R^2 = 0.958)	333.9 ± 21.9
1:1	12.7 ± 4.9	1.64 ± 0.33 (R^2 = 0.956)	249.1 ± 29.9

Data are mean ± SD, $n = 3$.

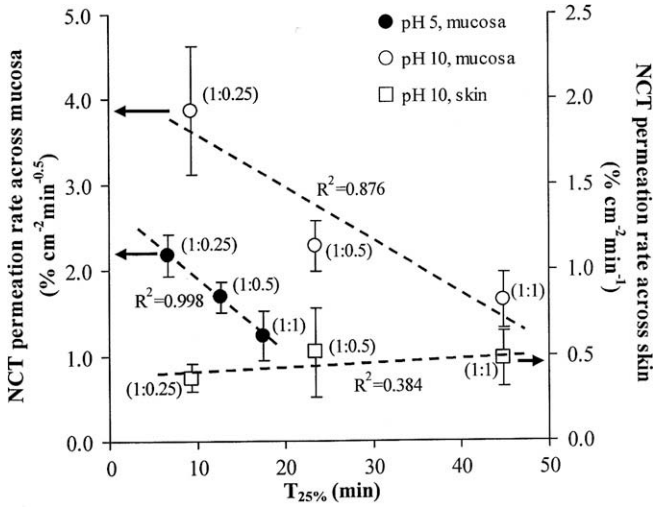

Fig. 7. Relationship between the $T_{25\%}$ value (NCT release rate) and NCT permeation rate across the skin and mucosa of NCT-loaded SA–MAS films using various SA–MAS ratios. The broken lines represent the regression lines and the SA–MAS ratio is presented in parentheses.

a slower NCT release of films with a higher ratio of MAS. Furthermore, the obvious relationship between mucosal membrane NCT permeation and the square root of time suggests that the permeation process was controlled by drug diffusion in the film matrix. In contrast to the results with skin as a barrier membrane, which presented a skin controlled mechanism described earlier, the mucosal membrane data indicate a matrix diffusion controlled mechanism.

The relationship between the $T_{25\%}$ value and NCT permeation rate across both shed snake skin and mucosal membrane is shown in Fig. 7. The data from the mucosal membrane show a clear relationship with the inverse proportion of both parameters. That is, the higher the $T_{25\%}$ value (which indicates a slower NCT release rate due to a greater MAS ratio in the films), the lower was the NCT permeation rate across the mucosal membrane. Additionally, the NCT-loaded SA–MAS films prepared at pH 10 gave higher permeation rates than those prepared at pH 5, although the pH 10 films had a slower NCT release rate when compared with the same SA–MAS ratios. This result was probably due to characteristics of the neutral NCT form in the films prepared at basic pH. On the other hand, both parameters of the films prepared at pH 10 had a poor correlation when using snake skin. This confirmed that the skin barrier acted as a rate-limiting step for NCT permeation.

3.6. Muco-adhesive properties of the films

The muco-adhesive properties of the films were successfully mimicked using the modified in-house instrument pulley system. The detachment force of the films is shown in Fig. 8. The NCT-loaded SA films prepared at pH 10 gave a higher detachment force than the NCT-loaded SA–MAS films. The detachment force tended to decrease with an increasing MAS ratio in the films. The preparation pH did not influence muco-adhesive properties of the films, similar to the results obtained in our previous study (Pongjanyakul & Suksri, 2009). It is well known that SA possesses a muco-adhesive property (Batchelor et al., 2002; Salamat-Miller, Chittchang, & Johnston, 2005; Sudhakar, Kuotsu, & Bandyopadhyay, 2006) because it contains many carboxyl and hydroxyl groups that can generate hydrogen bonds with other materials. It has been previously proposed that the interaction between the mucus on the mucosa and hydrophilic polymers occurs by physical entanglement and

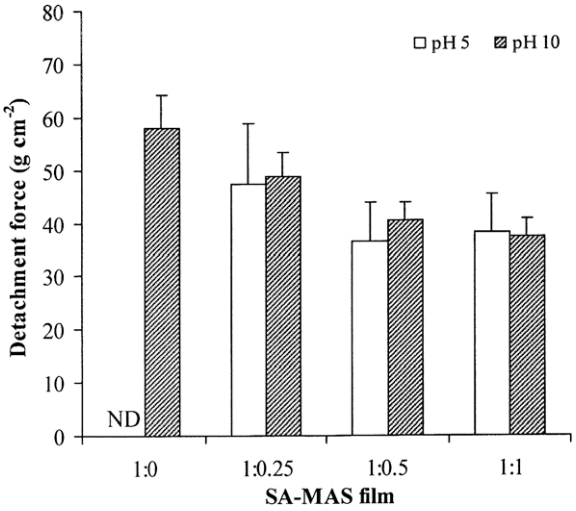

Fig. 8. Detachment force of NCT-loaded SA–MAS films prepared using various SA–MAS ratios at pH 5 and 10. Each value represents the mean ± SD of an $n = 6$.

chemical interactions, such as hydrogen bonding (Salamat-Miller et al., 2005). The change in pH to acidic conditions caused an increase in the unionized form of carboxyl groups of SA, though they could still create hydrogen bonding with mucin. This result may describe similarities in the detachment force of the films prepared at pH 5 and 10. Furthermore, interaction between the MAS with the hydroxyl and/or carboxyl groups of SA in the films (Pongjanyakul et al., 2005) caused a reduction in the amount of hydroxyl and/or carboxyl groups of SA available to interact with the mucus. This may lead to a lower muco-adhesive property of the NCT-loaded SA–MAS films. However, although the NCT-loaded SA–MAS films with SA–MAS ratio of 1:1 showed a twofold decrease in the amount of SA, the films could adhere to the mucosal membrane. Lavie and Stotzky (1986) reported that the montmorillonite clay can enhance the interaction between cells and particles. In addition, the higher cellular uptake efficiency was found when incorporated montmorillonite clay into nanoparticles (Dong & Feng, 2005). For these reasons, MAS, a silicate layer surface containing numerous hydroxyl groups, could possibly possess a muco-adhesive property with the mucosal membrane.

4. Conclusions

This study shows that the SA–MAS ratio influences the characteristics of NCT-loaded SA–MAS films. An increase in the MAS ratio caused a higher NCT retention and lowered the NCT release rate. The NCT release mechanism of the NCT-loaded SA–MAS films prepared at acidic and basic pH was influenced by both an anomalous transport and swelling controlled mechanism, respectively, which was impacted by the film SA composition. The NCT permeation rate across the mucosal membrane decreased with an increasing MAS ratio in the films and the drug permeation was a matrix diffusion controlled mechanism. Moreover, the films with a higher MAS ratio had sufficient muco-adhesive properties for adhesion to the mucosal membrane. The results of this study suggest that the NCT-loaded SA–MAS films show potential for mucosal drug delivery systems.

Acknowledgments

The authors would like to thank the Commission on Higher Education, the Ministry of Education (Bangkok, Thailand), and the Thailand Research Fund (Bangkok, Thailand) for research funding (Grant No. RMU4980022). We would also like to thank the Faculty of Pharmaceutical Sciences, Khon Kaen University (Khon Kaen, Thailand) for use of their technical facilities.

References

Adrian, C. L., Olin, H. B. D., Dalhoff, K., & Jacobsen, J. (2006). In vivo human buccal permeability of nicotine. *International Journal of Pharmaceutics, 311*, 196–202.

Aguzzi, C., Cerezo, P., Viseras, C., & Caramella, C. (2007). Use of clays as drug delivery systems: Possibilities and limitations. *Applied Clay Science, 36*, 22–36.

Alexandre, M., & Dubois, P. (2000). Polymer-layered silicate nanocomposites: Preparation, properties and uses of a new class of materials. *Materials Science and Engineering, 28*, 1–63.

Batchelor, H. K., Banning, D., Dettmar, P. W., Hampson, F. C., Jolliffe, I. G., & Craig, D. C. M. (2002). An in vitro mucosal model for prediction of bioadhesion of alginate solutions to the oesophagus. *International Journal of Pharmaceutics, 238*, 123–132.

Borodkin, P. B. (1993). Ion exchange resins and sustained release. In J. Swarbrick & J. C. Boylan (Eds.), *Encyclopedia of pharmaceutical technology* (Vol. 8, pp. 203–216). New York: Marcel Dekker Inc.

Campbell, K., Craig, D. Q. M., & McNally, T. (2008). Poly(ethylene glycol) layered silicate nanocomposites for retarded drug release prepared by hot-melt extrusion. *International Journal of Pharmaceutics, 363*, 126–131.

Chen, L. H., Chetty, D. J., & Chien, Y. W. (1999). A mechanistic analysis to characterize oramucosal permeation properties. *International Journal of Pharmaceutics, 184*, 63–72.

Cheng, Y. H., Watts, P., Hinchcliffe, M., Hotchkiss, R., Nankervis, R., Faraj, N. F., et al. (2000). Development of a novel nasal nicotine formulation comprising an optimal pulsatile and sustained plasma nicotine profile for smoking cessation. *Journal of Controlled Release, 79*, 243–254.

Diaz del Consuelo, I., Falson, F., Guy, R. H., & Jacques, Y. (2007). Ex vivo evaluation of bioadhesive films for buccal delivery of fentanyl. *Journal of Controlled Release, 122*, 135–140.

Diaz del Consuelo, I., Jacques, Y., Pizzolato, G., Guy, R. H., & Falson, F. (2005). Comparison of the lipid composition of porcine buccal and esophageal permeability barriers. *Archives of Oral Biology, 50*, 981–987.

Dong, Y., & Feng, S. (2005). Poly(D,L-lactide-*co*-glycolide)/montmorillonite nanoparticles for oral delivery of anticancer drug. *Biomaterials, 26*, 6068–6076.

Jung, H., Kim, H., Choy, Y. B., Hwang, S., & Choy, J. (2008). Itraconazole-laponite: Kinetics and mechanism of drug release. *Applied Clay Science, 40*, 99–107.

Kibbe, H. A. (2000). *Handbook of pharmaceutical excipients*. Washington: American Pharmaceutical Association.

Lavie, S., & Stotzky, G. (1986). Adhesion of the clay minerals montmorillonite, kaolinite, and attapulgite reduces respiration of *Histoplasma capsulate*. *Applied and Environmental Microbiology, 51*, 65–73.

Lee, C. H., Moturi, V., & Lee, Y. (2009). Thixotropic property in pharmaceutical formulations. *Journal of Controlled Release, 136*, 88–98.

Magalhães, N. F., & Andrade, C. T. (2009). Thermoplastic corn starch/clay hybrids: Effect of clay type and content on physical properties. *Carbohydrate Polymers, 75*, 712–718.

Mihranyan, A., Andersson, S. B., & Ek, R. (2004). Sorption of nicotine to cellulose powders. *European Journal of Pharmaceutical Sciences, 22*, 279–286.

Nair, M. A., Chetty, D. J., Ho, H., & Chien, Y. W. (1997). Biomembrane permeation of nicotine: Mechanistic studies with porcine mucosae and skin. *Journal of Pharmaceutical Sciences, 86*, 257–262.

Pavlidou, S., & Papaspyrides, C. D. (2008). A review on polymer-layered silicate nanocomposites. *Progress in Polymer Science, 33*, 1119–1198.

Peppas, N. A. (1985). Analysis of Fickian and non-Fickian drug release from polymers. *Pharmaceutica Acta Helvetiae, 60*, 110–111.

Pongjanyakul, T. (2009). Alginate–magnesium aluminum silicate films: Importance of alginate block structures. *International Journal of Pharmaceutics, 365*, 100–108.

Pongjanyakul, T., Khunawattanakul, W., & Puttipipatkhachorn, S. (2009). Physicochemical characterizations and release studies of nicotine–magnesium aluminum silicate complexes. *Applied Clay Science, 44*, 242–250.

Pongjanyakul, T., Prakongpan, S., Panomsuk, S., Puttipipatkhachorn, S., & Priprem, A. (2002). Shed king cobra and cobra skins as model membranes for in-vitro nicotine permeation studies. *Journal of Pharmacy and Pharmacology, 54*, 1345–1350.

Pongjanyakul, T., Priprem, A., & Puttipipatkhachorn, S. (2005). Investigation of novel alginate–magnesium aluminum silicate microcomposite films for modified-release tablets. *Journal of Controlled Release, 107*, 343–356.

Pongjanyakul, T., & Suksri, H. (2009). Alginate–magnesium aluminum silicate films for buccal delivery of nicotine. *Colloids and Surfaces B: Biointerfaces, 74*, 103–113.

Ritger, P. L., & Peppas, N. A. (1987). A simple equation for description of solute release. I. Fickian and non-Fickian release from non-swellable devices in the form of slabs, spheres, cylinders or discs. *Journal of Controlled Release, 5*, 23–36.

Salamat-Miller, N., Chittchang, M., & Johnston, T. P. (2005). The use of mucoadhesive polymers in buccal drug delivery. *Advanced Drug Delivery Reviews, 57*, 1666–1691.

Siepmann, J., & Siepmann, F. (2009). Mathematical modeling of drug delivery. *International Journal of Pharmaceutics, 364*, 328–343.

Sothornvit, R., Hong, S., An, D. J., & Rhim, J. (2010). Effect of clay content on the physical and antimicrobial properties of whey protein isolate/organo-clay composite films. *LWT – Food Science and Technology, 43*, 279–284.

Stephen, H. C., Mark Saltzman, W., & Giannelis, E. P. (2003). Organosilicate-polymer drug delivery systems: Controlled release and enhanced mechanical properties. *Journal of Controlled Release, 90*, 163–169.

Sudhakar, Y., Kuotsu, K., & Bandyopadhyay, A. K. (2006). Buccal bioadhesive drug delivery-a promising option for orally less efficient drugs. *Journal of Controlled Release, 114*, 15–40.

Suksri, H., & Pongjanyakul, T. (2008). Interaction of nicotine with magnesium aluminum silicate at different pHs: Characterization of flocculate size, zeta potential and nicotine adsorption behavior. *Colloids and Surfaces B: Biointerfaces, 65*, 54–60.

Tammaro, L., Costantino, U., Nocchetti, M., & Vittoria, V. (2009). Incorporation of active nano-hybrids into poly(ε-caprolactone) for local controlled release: Antifibrinolytic drug. *Applied Clay Science, 43*, 350–356.

Wan, L. S. C., & Prasad, K. P. P. (1989). Uptake of water by excipients in tablets. *International Journal of Pharmaceutics, 50*, 147–153.

Wang, X., Du, Y., Luo, J., Lin, B., & Kennedy, J. F. (2007). Chitosan/organic rectorite nanocomposite films: Structure, characteristic and drug delivery behaviour. *Carbohydrate Polymers, 69*, 41–49.

Wittaya-areekul, S., & Prahsarn, C. (2006). Development and in vitro evaluation of chitosan–polysaccharides composite wound dressings. *International Journal of Pharmaceutics, 313*, 123–128.